Acta Crystallographica Section D
Biological Crystallography
ISSN 0907-4449

Structure-based hypothesis on the activation of the CO-sensing transcription factor CooA

Mandula Borjigin,[a] Huiying Li,[a] Nicholas D. Lanz,[b] Robert L. Kerby,[b] Gary P. Roberts[b] and Thomas L. Poulos[a,c,d,e]*

[a]Department of Molecular Biology and Biochemistry, University of California, Irvine, California 92697, USA, [b]Department of Bacteriology, University of Wisconsin-Madison, Madison, Wisconsin 53706, USA, [c]Department of Physiology and Biophysics, University of California, Irvine, California 92697, USA, [d]Department of Chemistry, University of California, Irvine, California 92697, USA, and [e]The Center in Chemical and Structural Biology, University of California, Irvine, California 92697, USA

Correspondence e-mail: poulos@uci.edu

Received 28 September 2006
Accepted 28 November 2006

PDB Reference: CooA, 2hkx, r2hkxsf.

The CooA family of proteins are prokaryotic CO-sensing transcription factors that regulate the expression of genes involved in the utilization of CO as an energy source. They are homodimeric proteins that contain two hemes. Each monomer contains an N-terminal heme-binding domain and a C-terminal DNA-binding domain. Binding of CO to the heme leads to activation by a large reorientation of the DNA-binding domain such that the DNA-binding domain is in position for specific DNA recognition. The crystal structure of CooA from *Rhodospirillum rubrum* [RrCooA; Lanzilotta *et al.* (2000), *Nature Struct. Biol.* **7**, 876–880] in the inactive CO-free off-state shows that the N-terminal Pro residue of monomer *A* coordinates the heme of monomer *B* and *vice versa*. It now appears that the CO replaces the Pro ligand and that this change is coupled to the activation process. However, precisely how the replacement of the Pro ligand by CO results in structural changes some 25 Å from the CO-binding site remains unknown. Here, the structure of a CooA variant from the thermophilic bacterium *Carboxydothermus hydrogenoformans* (ChCooA) is reported in which one monomer is fully in the on-state. The N-terminal region that is displaced by CO binding is now positioned between the heme-binding and DNA-binding domains, which requires movement of the N-terminus by ∼20 Å and thus serves as a bridge between the two domains that helps to orient the DNA-binding domain in position for DNA binding.

1. Introduction

CooA is a CO-sensing transcription factor from the photosynthetic bacterium *Rhodospirillum rubrum* that belongs to the catabolite activator protein (CAP) family of prokaryotic transcription factors (Shelver *et al.*, 1995). Like CAP, CooA is a homodimeric protein, with each monomer consisting of an effector-binding and a DNA-binding domain which contains the classic helix–turn–helix DNA-binding motif. While cyclic AMP binds to the effector region in CAP, the effector domain in CooA binds heme, which in turn binds the effector molecule CO. The binding of CO to the heme promotes the binding of CooA to the 5′ promoter region of two operons, where CooA stimulates the transcription of genes responsible for CO oxidation (He *et al.*, 1996). This enables *R. rubrum* to utilize CO as an energy source (Kerby *et al.*, 1995; Ensign *et al.*, 1989).

While there are structures of CAP both with (Schultz *et al.*, 1991) and without (Passner *et al.*, 2000) DNA bound, all of these structures are in the DNA-binding on-state with the effector, cyclic AMP, bound. The structure of CooA provided the first picture of a CAP-like transcription factor in the off-state. Since CooA and CAP are structural homologues, the on-

state of CooA is expected to resemble the on-state of CAP. Therefore, a comparison between the off-state CooA and the on-state CAP structures provides insights into the range of motion induced by effector binding in each protein. Such a comparison shows that the DNA-binding domain undergoes a very large reorientation relative to the effector-binding domain upon activation. Although the two monomers of inactive CooA are in rather different orientations, they are both different from those of active CAP. Most importantly, the *F* helices of both monomers of inactive CooA, which make the critical sequence-specific DNA contacts, are oriented such that neither can bind DNA. As shown in Fig. 1, the *C* helices interact *via* a leucine-zipper motif and relative movement at the *C*-helical interface is thought to be involved in the activation process. In the crystal structure of CooA, the *C* helix of monomer *A* is fully extended, having fused the *C* and *D* helices (Fig. 1). In monomer *B* these helices are separated by a break, termed the hinge region, as in active CAP, but the relative position of the two domains is completely different in CooA monomer *B* compared with active CAP. It is thus apparent that the DNA-binding domains can undergo rather large changes in orientation relative to the effector-binding domain. An unexpected finding in the off-state RrCooA structure was that the N-terminal Pro residue of monomer *A* coordinates the heme of monomer *B* and *vice versa* (Lanzilotta *et al.*, 2000). It now appears that displacement of the Pro ligand by CO results in the off-to-on transition. However, precisely how displacement of the Pro ligand leads to large changes some 25 Å away remains unknown. The structure of ChCooA from *Carboxydothermus hydrogenoformans* that we report here differs from RrCooA in that one of the monomers has the DNA-binding domain in the on-state orientation. This provides a working hypothesis on a structural basis for how the displacement of the N-terminal ligand by CO results in the large reorientation of the DNA-binding domain required for DNA binding.

Table 1
Data-collection and refinement statistics.

Values in parentheses are for the outermost resolution shell.

Data set	MAD data (SSRL)			High-resolution data (ALS)
	Peak	Remote	Inflection	
PDB code				2hkx
Space group	$P2_12_12_1$			
Unit-cell parameters (Å)				
a	51.94	51.94	51.94	52.12
b	93.55	93.55	93.56	92.87
c	96.88	96.86	96.88	95.50
Data resolution (Å)	3.0	3.0	3.0	2.48
Total observations	67754	67052	67895	107917
Unique reflections	10081	9934	10092	15480
R_{sym}†	0.084 (0.829)	0.063 (0.492)	0.083 (0.846)	0.049 (0.43)
$\langle I/\sigma(I)\rangle$	8.0 (2.1)	9.9 (3.6)	7.9 (2.3)	11.1 (2.8)
Completeness (%)	99.7 (99.4)	99.6 (99.8)	99.6 (99.6)	93.3 (86.0)
Reflections used in refinement				19702
R factor‡				21.9
R_{free}§				28.7
No. of protein atoms				2966
No. of heteroatoms				45
No. of water molecules				58
R.m.s. deviation				
Bond lengths (Å)				0.016
Bond angles (°)				1.554
Average *B* factor (Å^2)				51

† $R_{sym} = \sum |I - \langle I\rangle| / \sum I$, where I is the observed intensity of a reflection and $\langle I\rangle$ is the averaged intensity of multiple observations of the reflection and its symmetry mates. ‡ *R* factor = $\sum ||F_o| - |F_c|| / \sum |F_o|$, where F_o and F_c are the observed and calculated structure factors, respectively. § R_{free} was calculated with the 5% of reflections set aside randomly throughout the refinement.

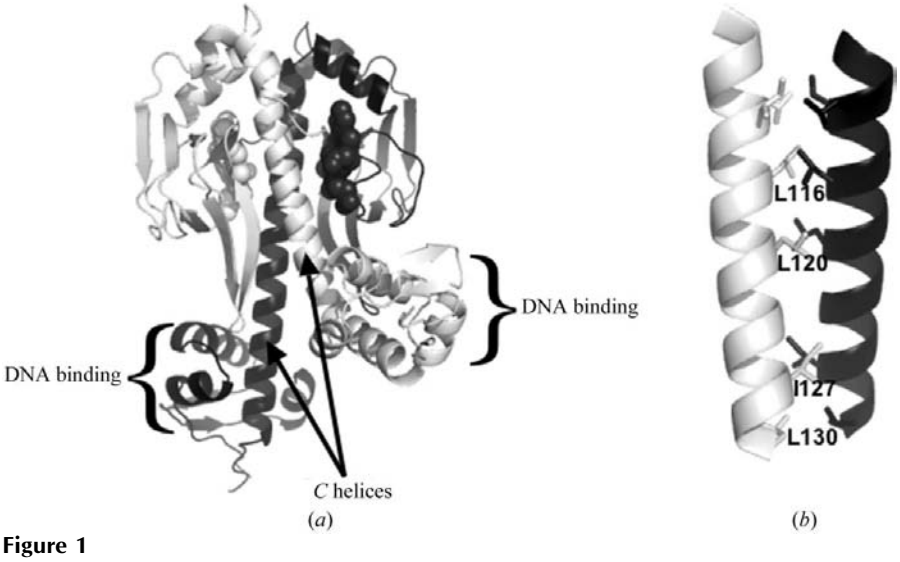

Figure 1
Crystal structure of RrCooA. (*a*) In monomer *A* (dark) the DNA-binding domain is in the fully extended orientation, while in monomer *B* (light) the DNA-binding domain is in a bent orientation. The van der Waals spheres are the heme groups. Note the long *C* helices that form the dimer interface. (*b*) A close-up view of the *C*-helical interface, showing the interaction between symmetry-related Leu and Ile residues.

2. Experimental procedures

2.1. Expression and purification

All ChCooA variants were expressed with C-terminal His tags in an *Escherichia coli* overexpression system as described previously (Clark *et al.*, 2006; Kerby *et al.*, 2003). Various mutants of both RrCooA and ChCooA have been generated as part of an effort to lock CooA in the on-state in order to facil-

itate structure solution of on-state CooA. Conversion of Asn127 and Ser128 of ChCooA to Leu was found to generate a mutant designated LL-ChCooA that is active in the absence of CO.

2.2. Crystallization and structural analysis

The purified protein was degassed and reduced with 2 m*M* sodium dithionite (DTH) anaerobically, followed by immediate removal of the DTH with a desalting column in 50 m*M* phosphate buffer pH 7.4, 500 m*M* KCl, 2 m*M* dithiothreitol (DTT). The protein sample was sealed in a serum vial and the air space was purged with CO gas. The protein was then concentrated to 558 µ*M* in a glove box. Crystals were grown inside the glove box by mixing equal volumes of the protein sample with reservoir solutions of 20% of PEG (polyethylene glycol) 4000, 0.1 *M* HEPES [4-(2-hydroxyethyl)-1-piperazine-ethanesulfonic acid] buffer pH 7.5 and 10% 2-propanol (Crystal Screen No. 41, Hampton Research Inc., Laguna Niguel, CA, USA). Rod-shaped crystals grew to full size (~0.1 × 0.15 × 0.7 mm) in a week, belong to space group $P2_12_12_1$ (unit-cell parameters a = 51.88, b = 93.10, c = 95.52 Å) and contain one homodimer in the asymmetric unit. A cryoprotectant solution was made by keeping all the components of the reservoir solution but increasing the 2-propanol content to 30%. The cryosolution was degassed and saturated with CO. Crystals were passed stepwise through cryosolutions with increasing amounts of 2-propanol in a glove box before being flash-cooled in liquid nitrogen.

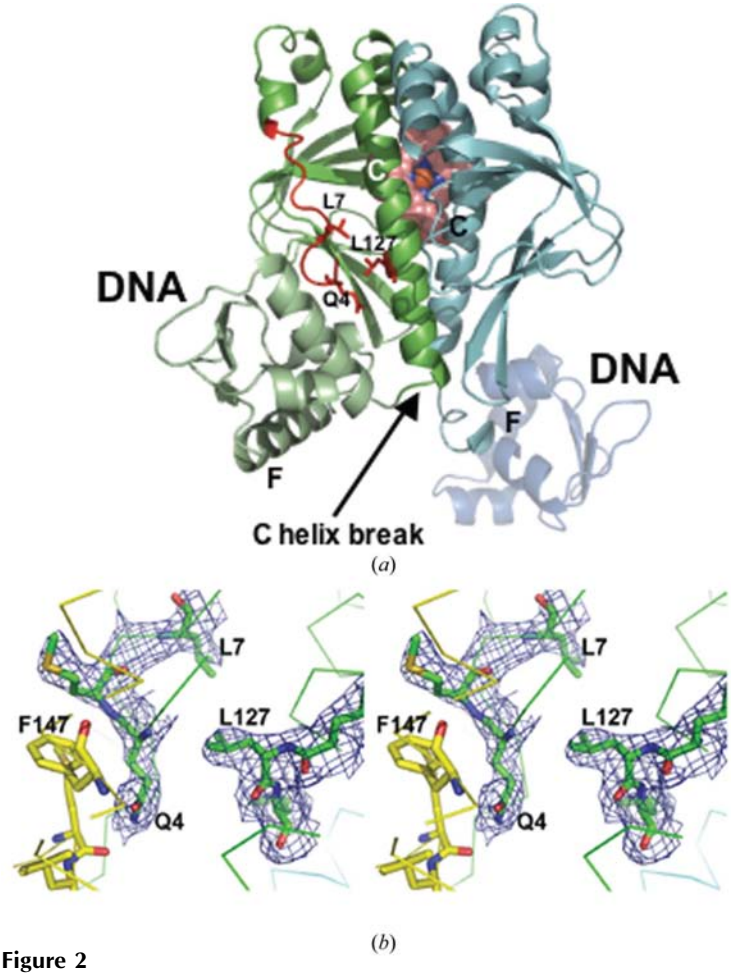

Figure 2
Structure of LL-ChCooA. (*a*) The monomer with heme bound is shown in green, while the heme-free monomer is shown in blue. Although the DNA-binding domain in the heme-free monomer is disordered, the first few helical turns in the DNA-binding domain are sufficiently well ordered to enable an approximate orientation of the DNA-binding domain. The DNA-binding *F* helix in each DNA-binding domain is labeled. Note that in the heme-bound monomer the *F* helix is oriented 'down' in position to bind DNA, while in the heme-free monomer the *F*-helix is oriented 'up'. The N-terminal segment of the heme-free monomer that is situated between the heme-binding and DNA-binding domains is shown in red. (*b*) Stereoview showing the $2F_o - F_c$ map contoured at 1σ of the N-terminal segment of monomer *A*. Residues of the heme-binding domain are shown in green and those of the DNA-binding domain are shown in yellow. Note that the introduced side chain of Leu127 interacts with Leu7, while Gln4 donates a hydrogen bond to the carbonyl O atom of Met177. The N-terminal segment thus serves as an intramolecular bridge between the heme-binding and DNA-binding domains.

A set of multiple-wavelength anomalous dispersion (MAD) data at three different wavelengths (1.7378, 1.653 and 1.7405 Å) and a set of high-resolution data (at an X-ray wavelength of 1.0 Å) were collected using two different crystals at beamline 1-5 at the Stanford Synchrotron Radiation Laboratory. The data were reduced with *DENZO* and *SCALEPACK* (Otwinowski & Minor, 1997) to yield a MAD data set at 3.0 Å resolution and high-resolution data at 2.3 Å. Additional data sets were also obtained at the Advanced Light Source, Lawrence Berkeley National Laboratory, one of which was used for the final structure refinement.

The structure was solved by MAD phasing. The single heme iron position was located using *SHELXD* (Schneider & Sheldrick, 2002) and was then fed into *SOLVE* (Schneider & Sheldrick, 2002) for phase refinement and *RESOLVE* (Terwilliger, 2003) for density modification. The electron-density map generated from *RESOLVE* was of interpretable quality (mean figure of merit = 0.41), showing all major α-helical and β-sheet structures. The model of RrCooA was manually overlaid onto the density as the starting model in *O* (Jones *et al.*, 1991). The density clearly indicated that the DNA-binding domain in ChCooA was in a different orientation from that in the RrCooA model, so this domain has to be repositioned independently. In the early stages of model building, the partial model phases were combined with the MAD phases using the programs *SFALL*, *SIGMAA* and *DM* from the *CCP*4 suite (Collaborative Computational Project, Number 4, 1994) in order to improve the density quality. Automated model building was attempted in *RESOLVE*, but only yielded some fragments owing to the limited data resolution (2.3 Å). The simulated-annealing protocol in *CNS* (Brünger *et al.*, 1998) was used to refine the initial partial models. The final refinements were then carried out with *REFMAC*, including TLS parameterization (Winn *et al.*, 2001)

using eight TLS groups for each of the two chains. The *TLS Motion Determination* web server (http://skuld.bmsc.washington.edu/~tlsmd/) was used to determine the optimal number of rigid bodies for the TLS refinements. The final statistics of data collection and model refinement are summarized in Table 1.

3. Results and discussion

A detailed characterization of the ChCooA variant LL-ChCooA will be published elsewhere (R. L. Kerby, N. D. Lanz, H. Youn and G. P. Roberts, submitted). Briefly, we found that conversion of Asn127 and Ser128 to Leu, creating LL-ChCooA, enables the double mutant to bind DNA in the absence of CO nearly as tightly as wild-type ChCooA in the presence of CO. Under the assay conditions used for analysis, LL-ChCooA with the iron in the Fe^{2+} state exhibits a K_d of $\sim$76 n*M* compared with $\sim$55 n*M* for wild-type CooA in the presence of CO. Wild-type ChCooA in the Fe^{2+} state without CO does not bind DNA. In addition, LL-ChCooA forms a CO complex that is stable for days at room temperature. Such stability is the main reason we chose to determine the crystal structure of LL-ChCooA in complex with CO.

The structure of LL-ChCooA is shown in Fig. 2. The heme from monomer *B* is missing and the DNA-binding domain of the heme-free monomer is disordered and not clearly visible in electron-density maps. However, immediately after the break in the *C* helix, the electron density for residues 136–149 is sufficiently clear to define the orientation of the first helix of the DNA-binding domain despite the relatively high average *B* factor of 91 Å^2 for these residues. This enables an approximate placement of the DNA-binding domain in the heme-free monomer (Fig. 2*a*). A disordered DNA-binding domain is not uncommon in this family of proteins. For example, we have obtained electron-density maps for various variants of RrCooA as well as CAP and in some cases the electron-density map for the DNA-binding domain is very weak. This reflects the inherent flexibility of the hinge region connecting the heme-binding and DNA-binding domains.

The absence of heme in monomer *B* is potentially more problematic, yet the absence of heme has essentially no effect on the structure of the heme-binding domain. The r.m.s. deviation of the heme-binding domain C^{α} atoms between monomers *A* and *B* is only 0.15 Å for 127 common C^{α} atoms.

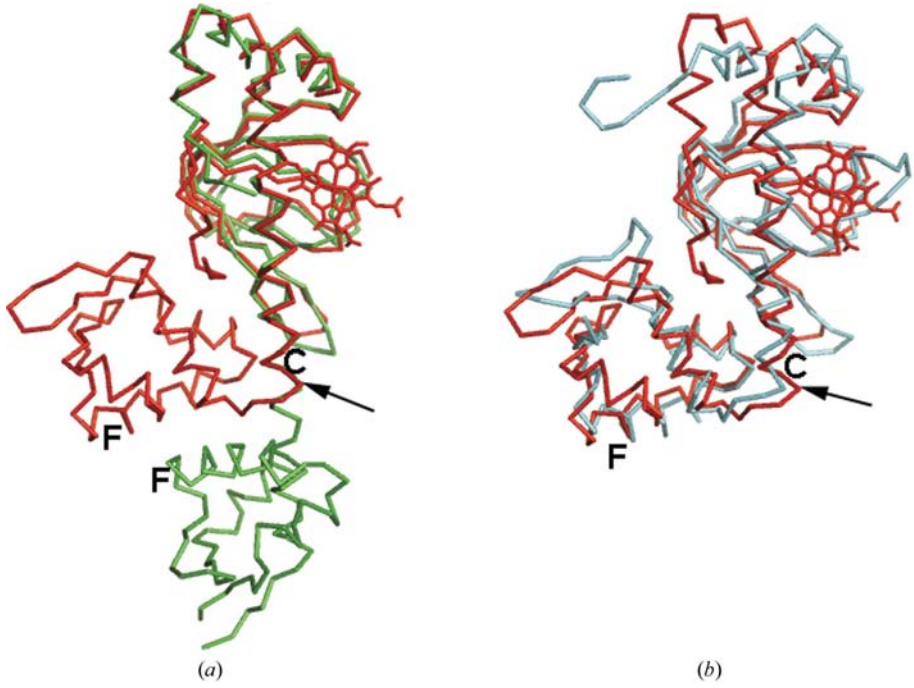

Figure 3
Models of LL-ChCooA compared with RrCooA and CRP. (*a*) Comparison of the heme-bound monomer of LL-ChCooA (red) with RrCooA (green). The arrow indicates the break in the *C* helix that enables the DNA-binding domain to reorient to the position compatible with DNA binding. (*b*) Comparison of LL-ChCooA (red) and CRP (blue). Note that the DNA-binding domains are both oriented in the active on-state. The *F* and *C* helices are labeled. The *F* helix in the DNA-binding domain forms specific interactions with DNA.

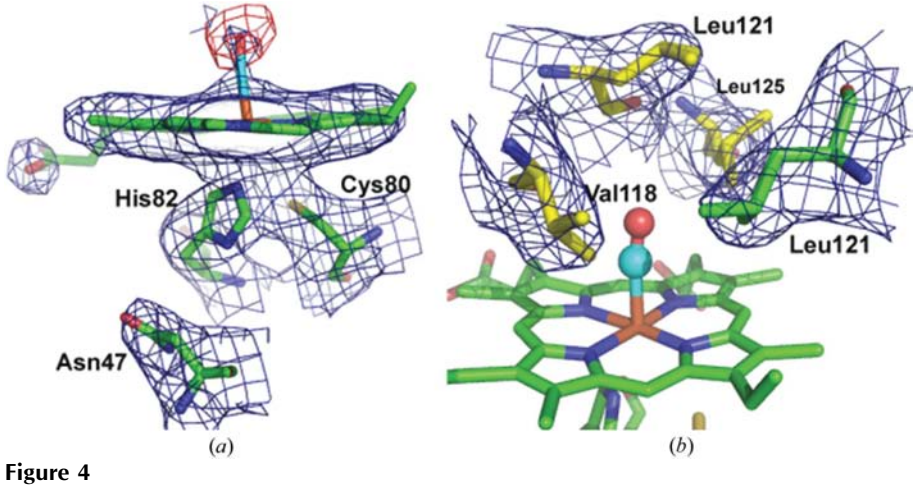

Figure 4
$2F_o - F_c$ electron-density map contoured at 1σ and $F_o - F_c$ map contoured at 3.0σ (red) around the heme site. (*a*) The electron densities for both Cys80 and His82 are continuous with the iron, although the geometry and the distance between Cys80 and the iron indicates very weak ligation. Also shown is Asn47 which in inactive RrCooA hydrogen bonds to the His ligand. However, in LL-ChCooA Asn47 is about 4.6 Å from His82. Both $2F_o - F_c$ and $F_o - F_c$ density indicate the presence of CO bound to the heme iron. (*b*) Structure around the CO-binding pocket. Residues shown in yellow are from molecule *B*, while those in green are from molecule *A*. The cluster of Leu residues forms a tight hydrophobic pocket around CO that favors a linear Fe—CO bond. Gly122 also contributes to the CO-binding pocket, but is not shown for clarity.

There is only a minor change in the heme-free monomer, where the His82 heme ligand rotates away from the heme pocket. Therefore, heme has little effect on the structure of the heme-binding domain.

The DNA-binding domain of monomer *A* that contains heme is in the on-state orientation, exactly the same as in CRP (PDB code 1j59; Figs. 3*a* and 3*b*), but is very different from off-state RrCooA (Fig. 3*a*) and thus represents the first on-state structure of a CooA. This is not unexpected since CO is bound to the heme iron as shown in Fig. 4(*a*). Although the heme is missing from monomer *B*, some insights into the changes in the heme pocket required for activation can be made by comparing the current LL-ChCooA CO-bound structure with the RrCooA off-state structure in addition to correlating these changes with those predicted from spectroscopic and mutagenic results. In LL-ChCooA the CO-binding pocket is much smaller than that in RrCooA. If we exclude the N-terminal ligand from RrCooA, the volume of the CO-binding pocket is 120 Å^3, compared with 92 Å^3 in LL-ChCooA. Using the *C* helix of molecule *A* as a stationary reference point, then the activation process involves removal of the N-terminal ligand and movement of the heme of molecule *A* and the *C* helix of molecule *B* such that a tight hydrophobic pocket for CO is formed (Fig. 4*b*). The steric restraints and hydrophobic nature of the CO pocket are also consistent with the ability of only CO and NO to activate wild-type ChCooA. The tight nonpolar pocket should exclude many potential ligands and the absence of hydrogen-bonding interactions would also explain the inability of O_2 to form a stable complex. O_2 prefers a bent geometry and the extensive mutagenesis data on myglogbin and data from model heme complexes show that a polar environment that can provide hydrogen bonds to the O_2 ligand is quite important in stabilizing the O_2 complex (Springer *et al.*, 1994). For example, changing the distal His in myoglobin to a nonpolar residue can change the O_2 off-rate by as much as 1000-fold (Springer *et al.*, 1994).

These changes are consistent with those predicted from mutagenic and spectroscopic studies. For example, Coyle *et al.* (2003) predicted that the RrCooA residues corresponding to Val118, Leu121 and Gly122 in LL-ChCooA would either contact CO or strongly influence CO binding and all of these residues fall in the immediate vicinity of CO. Similarly, the His77 heme ligand of RrCooA donates an hydrogen bond to Asn42 and resonance Raman data indicate that this bond is broken upon CO activation. The LL-ChCooA structure clearly shows that the corresponding His-Asn hydrogen bond is indeed broken (Fig. 4*a*). Coyle *et al.* (2003) also predicted that the N-terminal ligand is completely expelled from the heme pocket, which again is precisely what we find in the LL-ChCooA structure (Figs. 2*a* and 2*b*).

Perhaps the most striking feature of the new structure is the position of the ligand *trans* to His82 that is displaced by CO. In RrCooA Pro2 is the axial ligand in the inactive state, while for ChCooA it is generally thought that the N-terminal Met1 is the ligand. As noted above, it had been predicted that the N-terminus is displaced from the heme vicinity upon activation and the structure of LL-ChCooA provides an interesting hypothesis for its new location and a possible function. As shown in Fig. 2(*a*), the displaced N-terminal region of the heme-containing monomer is positioned between the effector-binding and DNA-binding domains. This raises the possibility that the N-terminal segment effectively stabilizes the on-state of the protein by stabilizing the proper relative position of these two domains. Specifically, Gln4 forms a hydrogen bond to the carbonyl O atom of Met177 in the DNA-binding domain and Leu7 is about 4 Å from the introduced Leu127, thus forming a hydrophobic patch (Fig. 2*b*). In the off-state of WT ChCooA, the surface-exposed Asn127 would be energetically more stable on the surface than an exposed Leu127 substitution. Therefore, LL-ChCooA has the additional energetic incentive to bury the introduced Leu127 side chain, which might provide additional stability to the on-state orientation of the DNA-binding domain. A schematic representation of the proposed CooA activation mechanism is shown in Fig. 5. During the review of this manuscript, one of the referees noted that since the heme-free monomer *B* also has a free N-terminal region, then one might expect monomer *B* to adopt the on-state conformation, although it does not. The reason is that in monomer *B* the N-terminus is oriented away from the main body of the protein, where it forms crystal contacts with a neighboring asymmetric unit and thus is not available to help hold the DNA-binding domain in the on-state orientation.

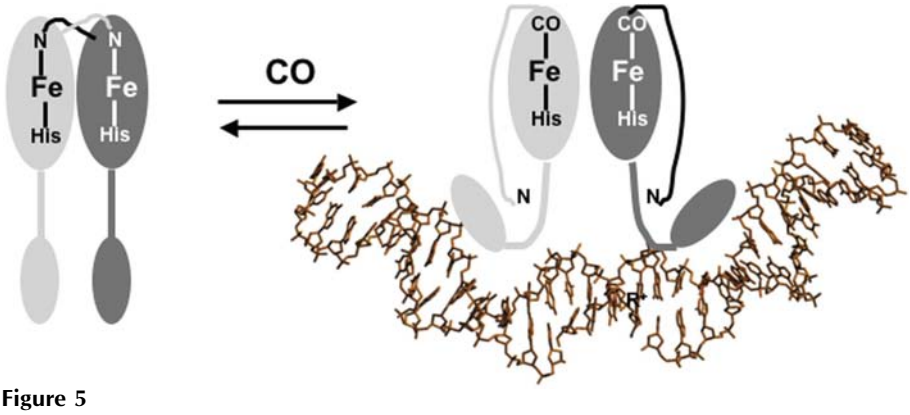

Figure 5
Proposed mechanism for CO sensing and activation by the CooA family of transcription factors. CooA is in an equilibrium mix between the off-state and on-state. In the off-state the N-terminus of monomer *A* coordinates the heme iron of monomer *B*. In the on-state the N-terminus dissociates, thus enabling CO to bind. The freed N-terminus undergoes a large repositioning that enables the N-terminal segment to provide a bridge between the heme-binding and DNA-binding domains, effectively holding the DNA-binding domain in the orientation required for DNA binding. These changes involve motion at the *C*-helical interface and heme which tightens the CO-binding pocket, thus providing additional stabilization to CO binding.

The most relevant available experimental data concern RrCooA variants altered in their N-terminal residues (Clark *et al.*, 2004). Clark and coworkers found that removal of the two residues near the N-terminus in RrCooA or the addition of one extra residue leads to a decrease in DNA-binding affinity by twofold to threefold. These data are not inconsistent with our proposed mechanism of CO activation. In LL-ChCooA, residue Met1 is not visible and removal of one extra residue should not grossly affect the interactions between the heme-binding and DNA-binding domains. In addition, one extra residue added to the N-terminus is easily accommodated.

An attractive feature of the model shown in Fig. 5 is that it provides a direct structural connection between changes in heme ligation and the repositioning of the DNA-binding domain some 20 Å away. A large movement of the CO-displaced N-terminal ligand from the heme pocket to the interface between the heme-binding and the DNA-binding domains provides the energetic incentive for the large re-orientation of the DNA-binding domain. This is likely to be a general mechanism for the CooA family of transcription factors, although sequence differences suggest that the specific interactions involving the N-terminal segment will differ.

4. Conclusions

The LL-ChCooA structure presented here is the first CooA structure in which the DNA-binding domain adopts the on-state orientation and the first with CO bound. Although the missing heme in monomer *B* has no effect on the structure of the heme-binding domain, we recognize that the missing heme generates some concern on the biological relevance of the new structure. Nevertheless, the LL-ChCooA structure has provided a structural basis for a working hypothesis on how CO binding leads to a reorientation of the DNA-binding domain. The key is what happens to the N-terminal region when the N-terminal ligand is displaced by CO. In the on-state monomer, the N-terminal region is situated between the DNA- and heme-binding domains, thus providing a 'glue' that helps to correctly orient the DNA-binding domain. The most appealing aspect of this hypothesis is its simplicity, which provides a direct connection between displacement of the N-terminal ligand by CO and reorientation of the DNA-binding domain.

This work was supported by the University of Wisconsin College of Agricultural and Life Sciences, NIH grant GM 53228 (to GPR) and NSF grant MCB0315283 and NIH grant GM42614 (to TLP).

References

Brünger, A. T., Adams, P. D., Clore, G. M., DeLano, W. L., Gros, P., Grosse-Kunstleve, R. W., Jiang, J.-S., Kuszewski, J., Nilges, M., Pannu, N. S., Read, R. J., Rice, L. M., Simonson, T. & Warren, G. L. (1998). *Acta Cryst.* D**54**, 905–921.

Clark, R. W., Lanz, N. D., Lee, A. J., Kerby, R. L., Roberts, G. P. & Burstyn, J. N. (2006). *Proc. Natl Acad. Sci. USA*, **103**, 891–896.

Clark, R. W., Youn, H., Parks, R. B., Cherney, M. M., Roberts, G. P. & Burstyn, J. N. (2004). *Biochemistry*, **43**, 14149–14160.

Collaborative Computational Project, Number 4 (1994). *Acta Cryst.* D**50**, 760–763.

Coyle, C. M., Puranik, M., Youn, H., Nielsen, S. B., Williams, R. D., Kerby, R. L., Roberts, G. P. & Spiro, T. G. (2003). *J. Biol. Chem.* **278**, 35384–35393.

Ensign, S. A., Bonam, D. & Ludden, P. W. (1989). *Biochemistry*, **28**, 4968–4973.

He, Y., Shelver, D., Kerby, R. L. & Roberts, G. P. (1996). *J. Biol. Chem.* **271**, 120–123.

Jones, T. A., Zou, J.-Y., Cowan, S. W. & Kjeldgaard, M. (1991). *Acta Cryst.* A**47**, 110–119.

Kerby, R. L., Ludden, P. W. & Roberts, G. P. (1995). *J. Bacteriol.* **177**, 2241–2244.

Kerby, R. L., Youn, H., Thorsteinsson, M. V. & Roberts, G. P. (2003). *J. Mol. Biol.* **325**, 809–823.

Lanzilotta, W. N., Schuller, D. J., Thorsteinsson, M. V., Kerby, R. L., Roberts, G. P. & Poulos, T. L. (2000). *Nature Struct. Biol.* **7**, 876–880.

Otwinowski, Z. & Minor, W. (1997). *Methods Enzymol.* **276**, 307–326.

Passner, J. M., Schultz, S. C. & Steitz, T. A. (2000). *J. Mol. Biol.* **304**, 847–859.

Schneider, T. R. & Sheldrick, G. M. (2002). *Acta Cryst.* D**58**, 1772–1779.

Schultz, S. C., Shields, G. C. & Steitz, T. A. (1991). *Science*, **253**, 1001–1007.

Shelver, D., Kerby, R. L., He, Y. & Roberts, G. P. (1995). *J. Bacteriol.* **177**, 2157–2163.

Springer, B. A., Sligar, S. G., Olson, J. S. & Phillips, G. N. (1994). *Chem. Rev.* **94**, 699–714.

Terwilliger, T. C. (2003). *Acta Cryst.* D**59**, 38–44.

Winn, M. D., Isupov, M. N. & Murshudov, G. N. (2001). *Acta Cryst.* D**57**, 122–133.